Korean J. Chem. Eng., **28**(2), 544-549 (2011)
DOI: 10.1007/s11814-010-0404-3

Mutation breeding of nuclease p1 production in *Penicillium citrinum* by low-energy ion beam implantation

Qinting He, Nan Li, Xiaochun Chen, Qi Ye, Jianxin Bai, Jian Xiong, and Hanjie Ying†

State Key Laboratory of Materials-Oriented Chemical Engineering, College of Biotechnology and Pharmaceutical Engineering, Nanjing University of Technology, Nanjing 210009, P. R. China
(*Received 30 March 2010 • accepted 16 August 2010*)

Abstract−Nuclease p1 is an important enzyme in the nucleotide industry that is used to hydrolyze nucleic acid into nucleotides. To improve enzyme activity, *Penicillium citrinum,* a nuclease p1 producing strain, was mutated by low-energy Nitrogen ion beam implantation at an energy level of 15 keV and a dose ranging from 1×10^{15}-1×10^{16} ions/cm^2. The mutant strain designated as N409 was obtained with a high yield of nuclease p1. The activity of nuclease p1 was 421 U/mL from the mutant strain N409, which was increased by 86% compared with the control. The fermentation kinetics of nuclease p1 by the mutant strain N409 was studied in a 30 L external airlifting bioreactor. A model was proposed using the logistic equation for microbial growth, the Luedeking-Piret equation for product formation and a Luedeking-Piret-like equation for substrate uptake. The results predicted from the model were in good agreement with the experimental observations.

Key words: Ion Beam Implantation, Mutation, *Penicillium citrinum*, Nuclease p1, Kinetic Model

INTRODUCTION

Nuclease p1 (EC 3.1.30.1) was first identified as a 5′-phosphodiesterase by Kuninaka et al. (1961) from *Penicillium citrinum*. The main function of this commercially available enzyme is to hydrolyze nucleic acid into four 5′-mononucleotides [1], which are widely used as food additives and pharmaceutical intermediates [2-4]. Interest in nuclease p1 is growing due to the wide application of these 5′-nucleotides [5]. However, the low activity of this enzyme constrains the nucleotide industry. A high yield nuclease p1 producing strain is imperative for the nucleotide industry [4].

Ion beam technology has previously been applied to special functions in semiconductors and in the surface modification of materials. It has been extended to the field of biology and agriculture since the discovery of rice mutation induced by 30 keV nitrogen implantation shown by a group of Chinese scientists [6]. As a new interdisciplinary subject, ion beam biotechnology [7] has been formed and rapidly developed in recent years. Ion beam implantation is regarded as a new mutation method in mutation induction in species of plants and industrial microbes [8-11]. Compared with conventional mutation methods, low-energy ion beam implantation has remarkable advantages, including a high mutation rate, wide mutation spectrum, and relatively low damage to the treated organisms [12]. Most importantly, this process is controllable since it is highly versatile as a result of careful selection of ions, energy and dosage to be implanted and the processing conditions [13]. Hence, ion beam implantation has become a successful mutation technique in industrial microbe breeding. To our knowledge, this is the rst investigation on mutation breeding of nuclease P1 production in *Penicillium citrinum* by low-energy ion beam technology.

†To whom correspondence should be addressed.
E-mail: yinghanjie@njut.edu.cn

In this study, we investigated the mutation of *Penicillium citrinum* induced by low-energy ion beam implantation and obtained mutant strains with higher nuclease p1 activity. We also studied the fermentation process in the mutant strains. Kinetic models were established to describe cell growth, enzyme production, and substrate utilization during fermentation in a 30 L external airlifting bioreactor. To the best of our knowledge, there are no reports on the application of ion beam implantation in *Penicillium citrinum* mutation research.

MATERIALS AND METHODS

1. Microorganism

The mutant strain N409 was selected from *Penicillium citrinum* YH-001 (isolated by our laboratory). Potato dextrose agar (PDA) slants were used for sporulation and storage.

2. Media and Culture Conditions

The culture was cultivated on the PDA slant at 28 °C for 6 days before it was inoculated into the fermentation medium.

The growth media composition was (per liter): 50 g of glucose, 5 g of peptone, 0.5 g of KH_2PO_4, 0.5 g of $K_2HPO_4{\cdot}3H_2O$, 0.4 g of $CaCl_2$, 0.4 g of $ZnSO_4$. The pH was adjusted to 6.5 before the medium was sterilized. One hundred mL of the medium was put into a 500 mL Erlenmeyer flask. All media were sterilized at 121 °C for 15 min. Fermentation was carried out at 28 °C in a rotary shaking incubator (250 rpm) for 24 h. The fermentation solution containing nuclease p1 was centrifuged at 8,000 rpm for 15 min at 4 °C, and the supernatant obtained was used as the nuclease p1 enzyme solution in subsequent studies.

3. Induction by Low Energy Ion Implantation

Following culture on PDA slants at 28 °C for 6 days, *Penicillium citrinum* conidia were selected, collected and a suspension was then prepared (ca. 108 conidia/mL). The conidia suspension (0.5 mL)

was evenly spread on a sheet of glass and desiccated at room temperature.

Ion beam implantation was performed at the Ion Beam Bioengineering Center, Nanjing University of Technology by using the heavy-ion implantation facility [14]. Nitrogen ion (N^+) with energy of 15 keV was chosen for ion bombardment. Ions were delivered at a dosage of 1×10^{15}-1×10^{16} ions/cm^2. The control without ion implantation was placed in the same target chamber. After ion beam bombardment, the *Penicillium citrinum* samples were cultured in PDA medium and the mutants obtained were tested for their nuclease p1 activity.

4. Biomass Determination

Biomass was determined by centrifuging 15 mL of fermentation solution for 10 min at 8,000 rpm. The supernatant was reserved for subsequent nuclease p1 activity assay. The mycelium was washed and dried at 105 °C for 24 h for hyphal dry-weight determination [15]. Each test was repeated three times to obtain a mean value for biomass and nuclease p1 activity.

5. Assay of Nuclease p1 Activity

Nuclease p1 activity was assayed by measuring the amount of acid-soluble nucleotides [1] produced by RNA hydrolysis catalyzed by nuclease p1. The enzyme solution (0.1 mL) was incubated with substrate solution (1 mL of 5% RNA (w/v), 0.9 mL of 0.2 M acetate buffer of pH 5.0, and 3 mM of Zn^{2+}) at 70 °C for 15 min. The reaction was stopped by adding 2.0 mL of ice-cold nucleic acid precipitator (0.25% ammonium molybdate dissolved in 2.5% perchloric acid, w/v). The mixture was settled in an ice-bath for 10 min. The precipitated RNA was removed by centrifugation at 10,000 rpm at 4 °C for 10 min. The supernatant was diluted 250-fold with distilled water. Absorbance of the diluted solution at 260 nm was read along with a blank without enzyme. The activity (U/mL) of the obtained nuclease p1 was calculated according to the following formula:

$$\text{Enzyme activity (U/mL)}=OD_{260}\times\alpha\times4.0\times250/(0.1\times15)=666.7\times\alpha\times OD_{260}$$

where α is a dilution factor of the enzyme before the enzyme activity assay.

One unit of enzyme activity is defined as the amount of enzyme that produces an increase in optical density of 1.0 in 1 min at 260 nm.

The protein concentration was determined by the method of Bradford (1976) using Coomassie Brilliant Blue G-250. The specific activity of nuclease p1 was calculated according to the following formula:

$$\text{Specific activity (U/mg)}=\text{nuclease p1 activity/protein concentration}$$

6. SDS-PAGE Analysis of the Enzyme Solution

Sodium dodecyl sulfate-polyacrylamide gel electrophoresis (SDS-PAGE) was carried out using BIORAD Powerpac 300 electrophoresis apparatus and the method of Laemmli (1970). Protein bands in the gel were visualized by Coomassie Brilliant Blue R-250 staining. The molecular mass of test proteins was compared with standard protein markers (β-galactosidase at 116 kDa, albumin at 66.2 kDa, glutamic dehydrogenase at 53 kDa, ovalbumin at 43 kDa, trypsin inhibitor at 20.1 kDa, and α-lactabumin at 14.4 kDa) purchased from Amersham Pharmacia, Biotech, UK.

7. Culture Conditions in the 30 L External Airlifting Bioreactor

Batch culture was performed in the 30 L external airlifting bioreactor (ALF-S005, Highke, China) containing 1.6 L of growth medium. The initial pH was 6.5. The aeration rate was regulated in the range 0.8 to 1.0 v/v/m. The operating temperature was controlled at 30 °C.

8. Kinetic Model

8-1. Microbial Growth

The logistic equation widely used in unstructured models for describing cell growth in batch fermentations was used [16,17]. This was a substrate independent model and described the inhibition of biomass on growth. The logistic equation was as follows:

$$\frac{dX}{dt}=\mu_m X\left(1-\frac{X}{X_m}\right) \tag{1}$$

where μ_m is the specic maximum growth rate with respect to the fermentation conditions. The integrated form of Eq. (1) using X= X_0 (t=0) gives a sigmoidal variation of X as a function of t which represents both an exponential and a stationary phase [Eq. (2)]:

$$X=\frac{X_0X_m e^{\mu_m t}}{X_m-X_0+X_0e^{\mu_m t}} \tag{2}$$

8-2. Product Formation

The kinetics of nuclease p1 formation is based on the Luedeking-Piret equation. This model was originally developed for the formation of lactic acid by *Lactobacillus delbrucckii* [18]. According to this model, the product formation rate depends upon both the instantaneous biomass concentration X, and growth rate dX/dt, in a linear manner:

$$\frac{dP}{dt}=\alpha\frac{dX}{dt}+\beta X \tag{3}$$

Substituting Eq. (2) in Eq. (3), integration yields the following equation:

$$P=\alpha X_0\left(\frac{X_m e^{\mu_m t}}{X_m-X_0+X_0e^{\mu_m t}}-1\right)+\beta\frac{X_m}{\mu_m}\ln\left(1-\frac{X_0}{X_m}(1-e^{\mu_m t})\right) \tag{4}$$

8-3. Substrate Uptake

Substrate utilization kinetics are usually expressed by the Luedeking-Piret-like equation which consists of both substrate consumption for maintenance and substrate conversion [19,20].

$$-\frac{dS}{dt}=\frac{1}{Y_{x/s}}\frac{dX}{dt}+\frac{1}{Y_{p/s}}\frac{dP}{dt}+m_s X \tag{5}$$

The amount of carbon substrate used for product formation was assumed to be negligible [20]; thus Eq. (5) could be changed as follows:

$$-\frac{dS}{dt}=\frac{1}{Y_{X/S}}\frac{dX}{dt}+m_s X \tag{6}$$

After substituting Eq. (2) into Eq. (6), the substrate utilization equation could be obtained as Eq. (7) by integrating:

$$S=S_0-\frac{X_0X_m e^{\mu_m t}}{Y_{X/S}(X_m-X_0+X_0X_m e^{\mu_m t})}+\frac{X_0}{Y_{X/S}}-\frac{X_m m_S}{\mu_m}\ln\frac{X_m-X_0+X_0e^{\mu_m t}}{X_m} \tag{7}$$

In this study, Eqs. (2), (4) and (7) were used to simulate the experi-

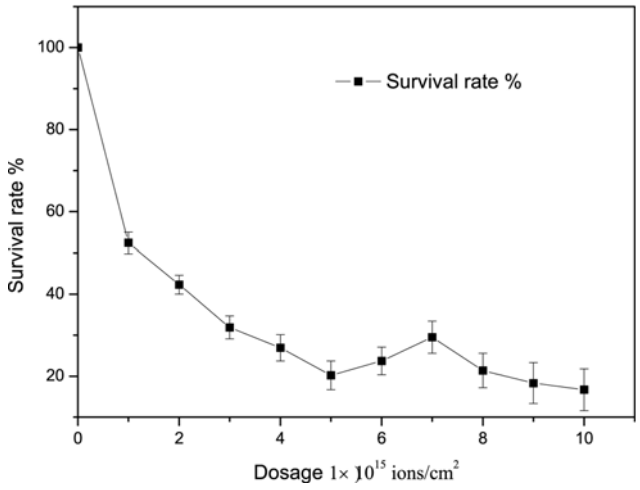

Fig. 1. Survival rate curve of *Penicillium citrinum* after ion beam implantation.

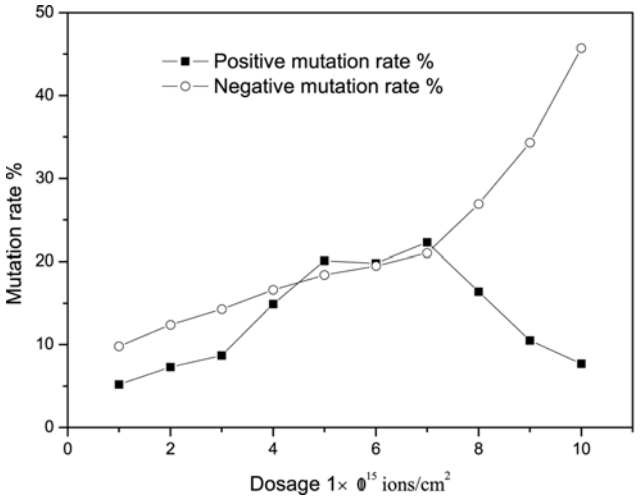

Fig. 2. The distribution of mutation rate after ion beam implantation.

mental results. The software Microcal Origin (Version 7.5, Microcal Software, MA 01060, USA) was employed to estimate the values of all the parameters.

RESULTS AND DISCUSSION

1. Optimum Parameter Determination of N^+ Implantation

Survival rate is correlated to the dose of N^+ implantation and shows a characteristic curve called the "saddle curve" [21] seen in Fig. 1. Initially, the survival rate decreased sharply with increased ion implantation dosage from 0 to 5×10^{15} ions/cm^2 and then increased slightly in the short range of 5-7×10^{15} ions/cm^2. Later, the survival rate continued to decrease as the dose increased. This tendency in the survival rate curve was in accordance with observations in reported experiments [9]. Within the dose range from 5×10^{15} ions/cm^2 to 7×10^{15} ions/cm^2, the abnormal change in the survival rate was different from those of other mutation methods such as UV irradiation and chemical treatment, which indicated that an abnormal repair mechanism in *Penicillium citrinum* conidia was induced by low energy ion beam implantation.

The mechanisms of low-energy ion implantation are not thoroughly understood. Yu proposed a hypothesis [22] in that the interaction between low-energy ions and the organisms is characterized by energy deposition, momentum transfer, mass deposition and charge neutralization and/or exchange. According to this hypothesis [23], there are four possible stages in the course of mutation. In the first stage, low dosage ions cause physical damage, such as micro-holes or crater-like structures, to the cell surface. In the second stage, the accelerated ions arrive at the inner part of cells through the holes in the cell membrane, which may directly act with DNA strands and lead to gene mutations. In this stage, most of the mutations are lethal to cells and the survival rate decreases sharply. In the third stage, the unclear repair mechanism is activated. Thus, the survival rate has a temporary rise. In the fourth stage, when the dosage of ions is further increased, the irradiation damage becomes irreparable.

According to the theory of Li [24], the optimum implantation dose was generally obtained at the turning points which were 5×10^{15} ions/cm^2 and 7×10^{15} ions/cm^2 in Fig. 1. However, verification of this by checking the positive mutation rate was crucial. The distribution of the both positive and negative mutation rate was obtained (Fig. 2). The mutants whose nuclease p1 activity was greater than 105% compared to the control were designated as positive mutation, whereas the mutants whose nuclease p1 activity was below 95% compared to the control were designated as negative mutation. The negative mutation rate was in line with the dose of ions implanted. However, the positive mutation rate was assumed to have normal distribution with its peak at the point of 7×10^{15} ions/cm^2 which decreased after that point. This result was in accordance with the theory of Cao et al. [25], which suggested that the optimum implantation dose was at the peak area. Hence, the optimum ion implantation dose in *Penicillium citrinum* conidia was at the energy value of 15 keV and a dosage of 7×10^{15} ions/cm^2.

2. Characteristics of Mutant N409

Following the determination of the optimum ion implantation conditions, the operation was repeated under the condition. The mutant N409 with nuclease p1 activity of 421 U/mL, which was 86% higher than that of the control, was obtained. This increase in activity may be due to the increase in yield of nuclease p1, or the increase in specific activity, or both. As shown in Table 1, after the determination of protein concentration by Bradford's method, the specific activities of nuclease p1 in the mutant strain and the control were 1,427 U/mg and 1,430 U/mg, respectively. The specific activity of nuclease p1 was almost constant in both the control and mutant N409, indicating that the enzymatic property was not altered following ion implantation. Therefore, it can be concluded that the increase in nuclease p1 activity was due to the higher yield rather than the change in enzymatic property.

Table 1. Specific activity of the control and mutant N409

Strain	Nuclease P1 activity (U/mL)	Protein concentration (mg/mL)	Specific activity (U/mg)
The control	226	0.1584	1427
Mutant N409	421	0.2944	1430

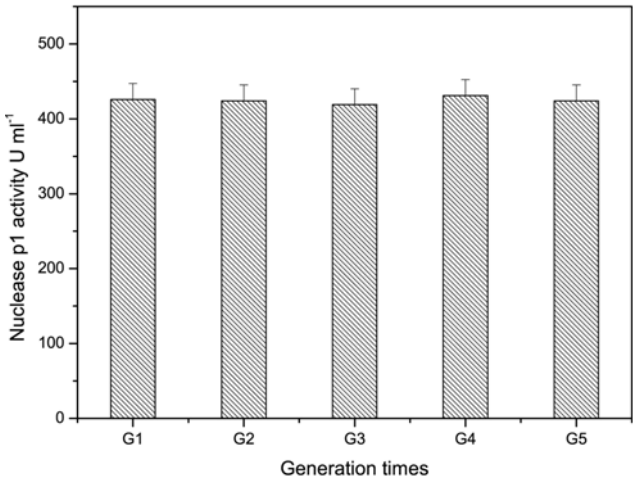

Fig. 3. Stability of mutant N409 during generations.

Mutant N409 was generated and inoculated into flask fermentations to test its stability in nuclease p1 activity (Fig. 3). It can be seen from the results that nuclease p1 activities remained relatively stable in subsequent generations, which suggested that the change was due to the inheritable mutation induced by ion beam implantation.

The constituents of the enzyme solution were determined by SDS-PAGE. Nuclease p1 based on a molecular weight of 44,000 [26] was consistent with the reference. Obviously, protein bands of nuclease p1 in some mutants after ion beam implantation were much more distinct than those of the control (Fig. 4). The number of enzyme bands was decreased such as in lane 3 (N409) and 4. The changes in the mutant strains might be caused by the ion mutant and effect the production of nuclease p1.

3. Kinetics of Batch Fermentation of Nuclease p1 in a 30 L External Airlifting Bioreactor

3-1. Fermentation Process

The batch growth profiles of mutant N409 with respect to biomass concentration, glucose concentration and the product are shown in Fig. 5. Three individual parallel experiments for each sample were carried out to obtain a more accurate result. The growth-curve of the mutant strain showed a classical growth trend, which was divided into four growth phases: lag, exponential, stationary and decline phases. After 8 h of lag time, cells were accumulated quickly and the maximum biomass concentration was obtained at 18 h. It was also observed that biomass growth was accompanied by the consumption of glucose (Fig. 5). The secretion of nuclease p1 was associated with cell growth. However, the rate of the increased enzyme activity was slower than that of the biomass growth. Maximum enzyme activity appeared in the decline phase, while the biomass was not increased. Therefore, product formation depended both on the cell growth rate and on the concentration of cells. The growth curve as seen in Fig. 5 was a typical sigmoidal according to the model of other microorganisms [27].

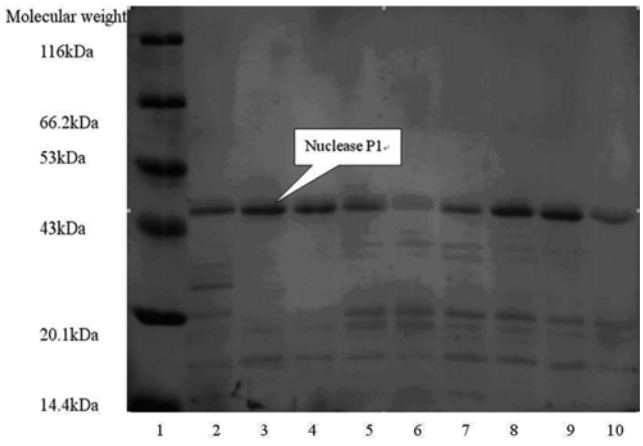

Fig. 4. SDS-PAGE analysis of enzyme solution (lanes: 1-protein molecular mass markers, 2-the control, 3-10-mutants after ion beam implantation).

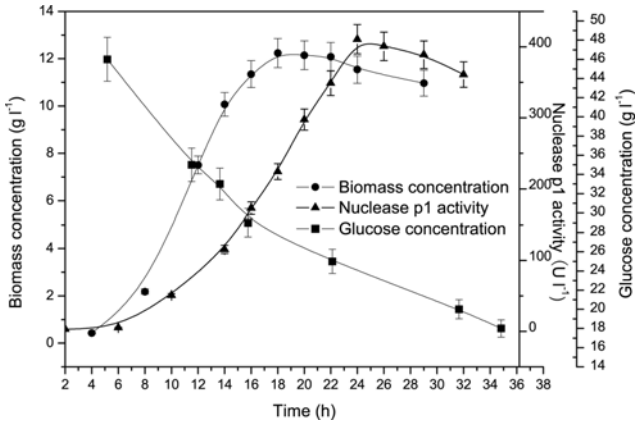

Fig. 5. Fermentation proles of *Penicillium citrinum* N409 in a 30 L external air-lift bioreactor.

3-2. Biomass Growth

By tting the experimental data to Eq. (2), the values for the parameters of biomass concentration were as follows: μ_m, X_0, and X_m were 0.497 h^{-1}, 0.050 g L^{-1} and 12.343 g L^{-1}, respectively. As shown in Fig. 6(a), the correlation coefficient (r^2) of the model was 0.999, which suggested that the t of the results was satisfactory.

3-3. Product Formation

The enzyme activity of nuclease p1 increased proportionally with the concentration of biomass in the exponential growth phase, and the production of enzyme continued to increase even during the stationary phase (Fig. 5). This suggested that the production of nuclease p1 by *Penicillium citrinum* followed the Luedeking-Piret model. The rate of product formation relied on both the rate of cell growth and the concentration of biomass [18]. Experimental data and the prediction by the kinetic model for nuclease p1 production are shown in Fig. 6(b). The r^2 of the model was 0.997. The growth-associated coefficient α and the non-growth-associated coefficient β for nuclease p1 production by *Penicillium citrinum* were estimated as in Fig. 6(b). The values of α and β were 1.217 and 2.500, respectively. According to the growth-associated coefficient and the non-growth-associated coefficient ($\alpha \neq 0, \beta \neq 0$), the nuclease p1 production model was consistent with fermentation process type II as classified by Gaden [28].

3-4. Substrate Uptake

In nuclease p1 fermentation, the increase in biomass concentration was accompanied by a decrease in residual glucose concentra-

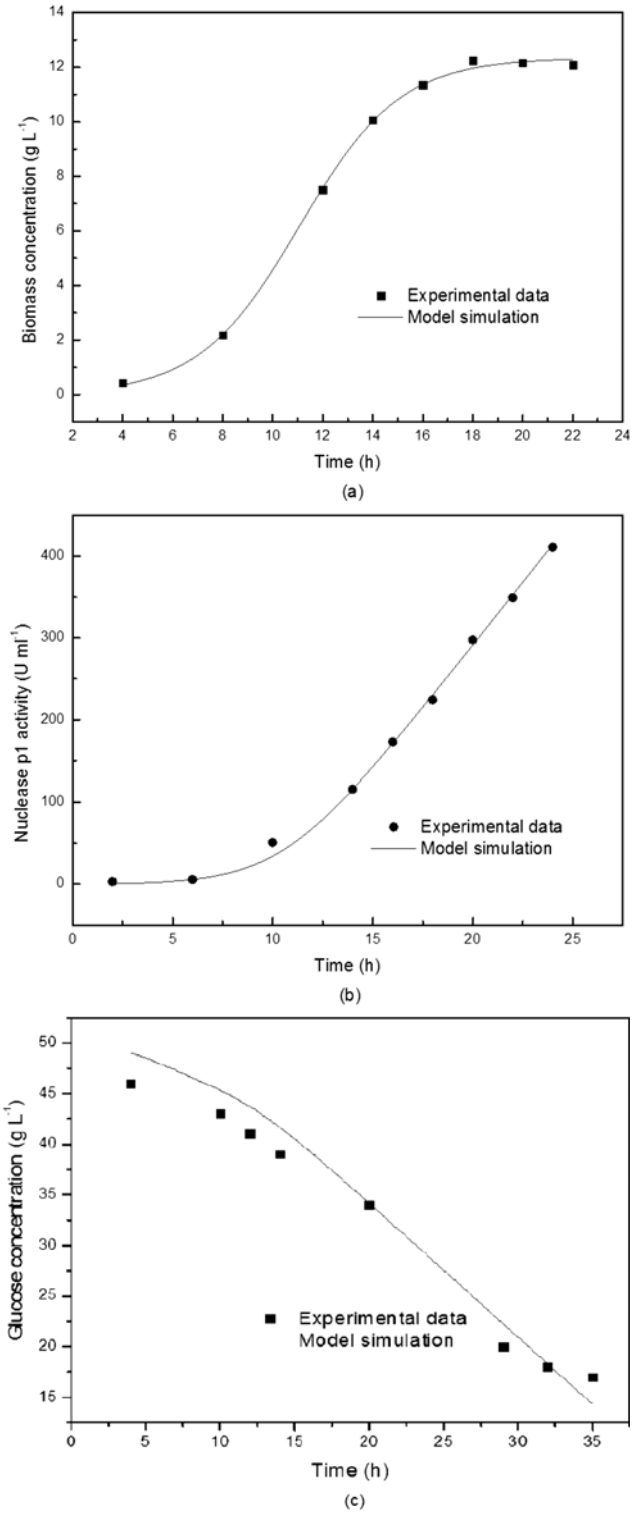

Fig. 6. Comparison of experimental data and kinetic model prediction of nuclease p1 batch production by *Penicillium citrinum* N409 in repeated batches of fermentation in a 30 L external air-lift bioreactor. The results are indicated by (a) bacterial growth, (b) nuclease p1 production, and (c) substrate utilization.

tion. The predicted evolutions of glucose concentration by Eq. (7) during the fermentation process are shown in Fig. 6(c). Together with the experimental data, this suggested that the prediction of the model agreed well with the experimental observations. The parameter r^2 of the model t was 0.959. The yield coefficient of biomass on the sugar, $Y_{X/S}$, was 0.24. The maintenance coefficient, m_s, was 0.11.

CONCLUSIONS

In this investigation with optimum energy (15 keV) and dose (7×10^{15} ions/cm^2), the mutant strain N409 was screened. The activity of nuclease p1 in the mutant strain N409 reached a level of 421 U/mL which was 86% higher than that of the parent strain. In addition, a kinetic model was developed for the batch production of the mutant strain. The model provided a good description of biomass, product and substrate concentrations with the logistic equation, Luedeking-Piret equation, and the Luedeking-Piret-like equation. The mutant strain had higher enzyme activities following low-energy ion beam implantation. A detailed description of the fermentation process would be helpful for the large scale production of nuclease p1.

ACKNOWLEDGEMENTS

This work was supported by the Major Basic R&D Program of China (2007CB707803), the National Key Technology R&D Program (2008BAI63B07), and the National Hi-Tech R&D Program of China (Grant No. 2006AA02Z236 and No. 2006AA020204). Qi YE was supported by the Innovation Fund for Doctoral Dissertation of Nanjing University of Technology (BSCX200911) and the Program (KJ103736).

NOMENCLATURE

m_s : maintenance coefficient [g sugar per g biomass h^{-1}]
P : produced nuclease p1 activity [U/mL]
S : glucose concentration [g L^{-1}]
S_0 : initial glucose concentration [g L^{-1}]
X : biomass concentration [g L^{-1}]
t : fermentation time [h]
X_0 : initial biomass concentration [g L^{-1}]
X_m : maximum biomass concentration [g L^{-1}]
$Y_{X/S}$: yield coefficient of biomass on glucose concentration [g per g sugar]
α : yield coefficient of nuclease p1 on biomass
β : non-growth-associated product formation coefficient
μ : specic growth rate [h^{-1}]
μ_m : specic maximum growth rate [h^{-1}]

REFERENCES

1. M. Fujimoto, A. Kuninaka and H. Yoshino, *Agric. Biol. Chem.*, **38**, 777 (1974).
2. L. K. Pickering, D. M. Granoff and J. R. Erickson, *Pediatrics*, **101**, 242 (1998).
3. K. Y. Chang and G. Varani, *Nat. Struct. Biol.*, **4**(Suppl.), 854 (1997).
4. G. Q. Ying, L. E. Shi and Y. Yu, *Process Biochem.*, **41**, 1276 (2006).
5. Z. J. Zhang, M. H. Wen and K. W. Wang, *Mod. Chem. Technol.*, **24**, 19 (2004).

6. Z. L. Yu, J. J. He and J. G. Deng, *AnHui Agric. Sci*., **28**, 12 (1989).
7. Z. L. Yu, *Surf. Coat Technol*., **201**, 8006 (2007).
8. X. Dai, Q. Huang and G. Li, *Plasma Sci. Technol*., **6**, 745 (2006).
9. N. Shikazono, Y. Yokota and S. Kitamura, *Genetics*, **163**, 1449 (2003).
10. D. Xu, Z. Zheng and P. Wang, *Plasma Sci. Technol*., **10**, 758 (2008).
11. Y. Chen, Z. X. Lin and Z. Y. Zou, *Nucl. Inst. Meth. Phys. Res*., **140**, 341 (1998).
12. B. Phanchaisri, R. Chandet and L. D. Yu, *Surf. Coat Technol*., **201**, 8024 (2007).
13. J. Oñate, F. Alonso and A. García, *Thin Solid Films*, **317**, 471 (1998).
14. W. D. Huang, Z. L. Yu and Y. H. Zhang, *Chem. Phys.*, **237**, 223 (1998).
15. T. L., *Process Biochem.*, **28**, 467 (1993).
16. R. M. Weiss and D. F. Ollis, *Biotechnol. Bioeng*., **22**, 859 (1980).
17. F. García-ochao and J. A. Casas, *Enzyme Microb. Technol*., **25**, 6139 (1999).
18. R. Luedeking and E. L. Piret, *J. Biochem. Microbiol. Technol. Eng.*, **1**, 393 (1959).
19. J. Z. Liu, L. P. Weng and Q. L. Zhang, *Biochem. Eng. J*., **14**, 137 (2003).
20. M. Elibol and F. Mavituna, *Process Biochem*., **34**, 625 (1999).
21. C. X. Su, W. Zhou and Y. H. Fan, *J. Ind. Microbiol. Biotechnol*., **33**, 1037 (2006).
22. N. Zhang and L. Yu, *Plasma Sci. Technol*., **11**, 110 (2009).
23. Z. L. Yu, *Anhui Sci. Technol.*, Press, Hefei (1998).
24. S. C. Li, M. Wu and J. M. Yao, *Plasma Sci. Technol*., **7**, 2697 (2005).
25. X. H. Cao, B. B. Du and M. F. Lu, *J. Chinese Inst. Food Sci. Technol*., **5**, 128 (2005).
26. M. Fujimoto, A. Kuninaka and H. Yoshino, *Agric. Biol. Chem.*, **39**, 1991 (1975).
27. M. R. Marín, *Am. J. Enol. Viticult*, **50**, 166 (1999).
28. J. R. Gaden, *J. Biochem. Microbiol. Technol. Eng.*, **1**, 413 (1959).